doubly transgenic population was not extended significantly ($N = 6$, $\bar{X} = 189.5 \pm 43.4$, $P > 0.05$). Thus, neither the proximal axonal cytopathology nor the clinical course of the SOD1 disease were modulated by either the NFHlacZ-mediated deficiency of axonal neurofilaments or the simultaneous accumulation of neurofilaments in motor neuron perikarya.

For the two mouse models of neuronal disease investigated here, neither initiation nor progression of pathology requires an axonal neurofilament cytoskeleton. This circumstance suggests that the neurofilament perturbations observed in these diseases arise as a passive response contributing little or nothing to the pathogenesis. It remains to be determined if and how far this conclusion can be generalized to human disease. The disparity between humans and rodents in both axon lengths and lifespan makes comparison of respective disease courses difficult. In addition, the possibility that interspecific amino-acid substitutions or additional genetic variation in neurofilament proteins may contribute to the pathogenesis of sporadic forms of ALS is the subject of debate[29,30]. The resolution of these issues will be of particular significance in dissecting the pathogenic mechanisms underlying the many human late-life neurodegenerative conditions that exhibit abnormal neurofilament accumulations. □

Methods

Transgenic mice. NFHlacZ transgenic mice[18] bear a fusion gene composed of mouse NFH, truncated in the forth exon (EcoRV) and ligated in frame to bacterial LacZ. The dt allele used throughout this investigation resulted from insertion, within the dt gene, of a hsplacZ construct[23]. Three lines of SOD1 mice (lines 9, 29 and 42), in which different levels of the human G37R mutant SOD1 protein accumulate[17], were evaluated in this study. All animals were carefully monitored for onset and progression of disease. From the moment signs of weakness became apparent, a slow evolution to greater weakness occurred which was followed by a phase of rapid clinical deterioration. When the locomotion of affected animals became compromised they were considered to be in end-stage disease and were killed. Longevity results were compared by T-test.

Crosses were performed between (dt/+, NFHlacZ/−) and (dt/+, −/−) mice such that individual litters contained (dt/dt, −/−) and (dt/dt, NFHlacZ/−) mice as well as unaffected transgenic and non-transgenic mice. For SOD1, littermates derived from crossing mutant SOD1/+ and NFHlacZ/+ mice were compared. The genotype of each animal was determined by polymerase chain reaction (PCR). For NFHlacZ primers (5′-AGGCTGCATCT CCA-GAAAAAGAAACC-3′) and (5′TCATCATTAAAGCGAGTGGCAACA-3′) were used. For dt we used: (5′-GATCCTGTGAGACGGGAGAATGT-3′) and (5′-CACCTTGCTGAGGCAGGCTCTCC-3′), and for SOD1: (5′-CCAAGAT GCTTAACTCTTGTAATCAATGGC-3′) and (5′-CAGCAGTCTCATTGCCCA GGTCTCCAACATG-3′).

Electron microscopy and axon counts. Mice were anaesthetized with avertin ($8 \, \text{mg kg}^{-1}$) and perfused transcardially with 0.5% paraformaldehyde, 2.5% glutaraldehyde in 0.1 M phosphate buffer at room temperature (pH 7.4). Tissues were dissected and left in the same fixative overnight. After a brief rinse in 0.1 M phosphate buffer, the samples were post-fixed in 1% osmium tetroxide for 1 h, washed in 0.1 M phosphate buffer, and dehydrated in ethanol. The tissues were embedded in Epon, and sectioned for light or electron microscopy. Sections were stained with toluidine blue for light microscopy, and lead citrate and uranyl acetate for electron microscopy (JEOL 100 electron microscope).

To count the number of myelinated axons in each spinal root, a montage of the complete root was prepared using NIH Image software and an Olympus microscope (×100 objective) connected to a Macintosh PowerPC 7500 by a video camera. The number of myelinated axons was counted on each montage. To count the number of ventral root fibres undergoing wallerian degeneration, cross-sections were observed at ×630 with DIC optics using a Zeiss Axiophot microscope.

1. Dickson, D. W. et al. Ballooned neurons in select neurodegenerative diseases contain phosphorylated neurofilament epitopes. Acta Neuropathol. **71,** 216–223 (1986).
2. Goldman, J. E. & Yen, S. H. Cytoskeletal protein abnormalities in neurodegenerative diseases. Ann. Neurol. **19,** 209–223 (1987).
3. Carden, M. J., Lee, V. M.-Y. & Schlaepfer, W. W. 2,5-Hexanedione neuropathy is associated with covalent crosslinking of neurofilament proteins. Neurochem. Pathol. **5,** 25–35 (1986).
4. Eyer, J., McLean, W. G. & Leterrier, J. F. Effect of a single dose of β,β′-Iminodipropionitrile in vivo on the properties of neurofilaments in vitro: comparison with the effect of Imminodipropionitrile added directly to neurofilaments in vitro. J. Neurochem. **52,** 1759–1765 (1989).
5. Pollanen, M. S., Dickson, D. W. & Bergeron, C. Pathology and biology of the Lewy body. J. Neuropathol. Exp. Neurol. **52,** 183–191 (1993).
6. Hill, W. D., Lee, V. M.-Y., Hurtig, H., Murray, J. M. & Trojanowski, J. Q. Epitopes located in spatially separate domains of each neurofilament subunit are present in Parkinson's disease Lewy body. J. Comp. Neurol. **109,** 150–160 (1991).
7. Griffin, J. W. & Price, D. L. in Experimental and Clinical Neurotoxicology (eds Spencer, P. & Schaumburg, H. H.) 161–178 (Williams and Wilkins, Baltimore, 1980).
8. Carpenter, S. Proximal axonal enlargement in motor neuron disease. Neurology **18,** 841–851 (1968).
9. Lee, M. K. & Cleveland, D. W. Neurofilament function and dysfunction: involvement in axonal growth and neuronal disease. Curr. Opin. Cell Biol. **6,** 34–40 (1994).
10. Coté, F., Collard, J. F. & Julien, J. P. Progressive neuronopathy in transgenic mice expressing the human neurofilament heavy gene: a mouse model of amyotrophic lateral sclerosis. Cell **73,** 35–46 (1993).
11. Lee, M. K., Marszalek, J. R. & Cleveland, D. W. A mutant neurofilament subunit causes massive, selective motor neuron death: implications for the pathogenesis of human motor neuron disease. Neuron **13,** 975–988 (1994).
12. Xu, Z. H., Cork, L. C., Griffin, J. W. & Cleveland, D. W. Increased expression of neurofilament subunit NF-L produces morphological alterations that resemble the pathology of human motor neuron disease. Cell **73,** 23–33 (1993).
13. Cleveland, D. W. et al. Mechanisms of selective motor neurons death in transgenic mouse models of motor neuron disease. Neurology **47,** 54–61 (1996).
14. Yang, Y. et al. An essential cytoskeletal linker protein connecting actin microfilaments ot intermediate filaments. Cell **86,** 655–665 (1996).
15. Brown, A., Bernier, G., Mathieu, M., Rossant, J. & Kothary, R. The mouse dystonia musculorum gene is a neural isoform of bullous pemphigoid antigen 1. Nature Genet. **10,** 301–306 (1995).
16. Rosen, D. R. et al. Mutations in Cu/Zn superoxide dismutase gene are associated with familial amyotrophic lateral sclerosis. Nature **362,** 59–62 (1993).
17. Wong, P. C. et al. An adverse property of a familial ALS-linked SOD1 mutation causes motor neuron disease characterized by vacuolar degeneration of mitochondria. Neuron **14,** 1105–1116 (1995).
18. Eyer, J. & Peterson, A. C. Neurofilament-deficient axons and perikaryal aggregates in viable transgenic mice expressing a neurofilament-β-galactosidase fusion protein. Neuron **12,** 389–405 (1994).
19. Plummer, J., Peterson, A. & Messer, A. Accelerated and widespread neuronal loss occurs in motor neuron degeneration (MND) mice expressing a neurofilament-disrupting transgene. Mol. Cell. Neurosci. **6,** 532–543 (1995).
20. Tu, P.-H. et al. Selective degeneration of Purkinje cells with Lewy body-like inclusions in aged NFHlacZ transgenic mice. J. Neurosci. **17,** 1064–1074 (1997).
21. Guo, L. et al. Gene targeting of BPAG1: abnormalities in mechanical strength and cell migration in stratified squamos epithelia and severe neurologic degeneration. Cell **81,** 233–243 (1995).
22. Duchen, L. W. Dystonia musculorum: an inherited disease of the nervous system in the mouse. Adv. Neurol. **14,** 353–365 (1976).
23. Kothary, R. et al. A transgene containing lacZ inserted into the dystonia locus is expressed in neural tube. Nature **335,** 435–437 (1988).
24. Campbell, R. M. & Peterson, A. C. An intrinsic neuronal defect operates in dystonia musculorum: a study of dt/dt ↔ +/+ chimeras. Neuron **9,** 693–703 (1992).
25. Sotelo, C. & Guenet, J. F. Pathologic changes in the CNS of dystonia musculorum mutant mouse: an animal model for human spinocerebellar ataxia. Neuroscience **27,** 403–424 (1988).
26. Gurney, M. E. et al. Motor neuron degeneration in mice that express a human Cu, Zn superoxide dismutase mutation. Science **264,** 1772–1775 (1994).
27. Beckman, J. S., Carson, M., Smith, C. D. & Koppenol, W. H. ALS, SOD and peroxynitrite. Nature **364,** 584 (1993).
28. Collard, J.-F., Cote, F. & Julien, J. P. Defective axonal transport in a transgenic mouse model of amyotrophic lateral sclerosis. Nature **375,** 61–64 (1995).
29. Figlewicz, D. et al. Variant alleles of the neurofilament heavy gene associated with amyotrophic lateral sclerosis. Hum. Mol. Genet. **3,** 1757–1761 (1994).
30. Vechio, J., Bruijn, L., Brown, R. & Cleveland, D. Sequence variants in human neurofilament proteins: absence of linkage ot familial amyotrophic lateral sclerosis. Ann. Neurol. **40,** 603–610 (1996).

Blocking apoptosis prevents blindness in *Drosophila* retinal degeneration mutants

Florence F. Davidson* & **Hermann Steller**

Howard Hughes Medical Research Institute, Massachusetts Institute of Technology, 31 Ames Street, Cambridge, Massachusetts 02139, USA

Apoptosis is a gene-directed form of cell death that is essential for normal development and health. Yet abnormally high levels of apoptosis are linked to many degenerative diseases[1]. Some important biochemical events in apoptosis have been identified[2], but the therapeutic utility of blocking cell death remains unclear. An important question in this regard is whether cells rescued from

* Present address: Department of Biochemistry, National Institutes of Health, National Cancer Institute, Bethesda, Maryland 20892, USA.

apoptosis can function. We have investigated the mechanism of cell death in two *Drosophila* mutant strains that exhibit age-related retinal degeneration. One of these mutations also occurs in humans, where it causes retinitis pigmentosa. We found that retinal cell death in *rdgC* and *ninaE*[RH27]/+ flies occurred by apoptosis and was blocked by eye-specific expression of the baculoviral cell survival protein p35. Most importantly, the mutant flies expressing p35 showed significant retention of visual function. The results demonstrate a therapeutic benefit of late-stage inhibition of apoptosis to flies, and suggest that similar results may be obtained in higher organisms.

Age related retinal degenerations, including retinitis pigmentosa (RP) are a leading cause of human blindness. In these diseases, initially functional photoreceptor cells of the eye are irreplaceably lost over time. There are two main mechanisms by which cells can die: necrosis, which is a lytic response to overwhelming stress, and apoptosis. Apoptosis is non-lytic, morphologically distinct, and its core elements are apparently conserved in all cells[2–4,29]. Previous results indicate that cell death in rodent models of RP is apoptotic[5–7]. About 30% of all autosomal dominant RP is caused by mutations in the photoreceptor protein rhodopsin[8], and equivalent mutations in the rhodopsin gene of *Drosophila* photoreceptor R1-6 cells also cause dominant, age-related retinal degeneration[9,10]. This suggests that the activation of cell death by such mutations occurs by a common mechanism, despite downstream differences in fly and human phototransduction pathways. The *Drosophila* strain *ninaE*[RH27] carries a dominant rhodopsin 1 mutation, C200Y (ref. 10), whose equivalent in humans causes severe RP[11]. Retinal degeneration in heterozygous *ninaE*[RH27] flies begins at about 3

weeks of age[10]. The *rdgC*[306] strain carries a deletion of a serine/threonine protein phosphatase that appears to dephosphorylate light-activated rhodopsin[12–14]. Retinal degeneration in homozygous *rdgC*[306] flies begins after 2 days in constant light. There is no known analogy to the *rdgC*[306] mutation in humans, but mutations near the phosphorylation sites of human rhodopsin are known to cause autosomal dominant RP[15].

We examined the morphology of dead and dying cells in *ninaE*[RH27]/+ and *rdgC*[306] fly retinas to determine whether death was by apoptosis. Figure 1 shows representative electron micrographs of wild-type and *ninaE*[RH27]/+ fly retinas. Fly eyes are composed of symmetrically repeating cell clusters, or ommatidia. A typical cross-section of a wild-type ommatidium, in which the six peripheral photoreceptor cells (R1–6) can be seen enclosing a central photoreceptor cell (R7 here), is shown in Fig. 1a. Some of the pigment cells that separate each ommatidium are seen at the periphery. The morphology of a representative *ninaE*[RH27]/+ ommatidium after light-rearing for 8 weeks is shown in Fig. 1b. At this age, the cell bodies of all remaining R1–6 cells were small and the rhabdomere membranes reduced and disorganized. The cells showed the typical features of apoptosis: cytoplasmic condensation, nuclear chromatin condensation, and relatively normal looking mitochondria (Fig. 1d, e). Electron-microscopic examination of degenerating *rdgC*[306] retinas also revealed these features of apoptosis after 11 days in the light (not shown).

A common feature of apoptosis is the activation of cysteine proteases known as caspases[16]. The baculoviral cell survival factor p35 inhibits a broad spectrum of these[17,18] and blocks apoptosis in insects[19–22], nematodes[17,23] and mammalian cells[24–26]. To test the
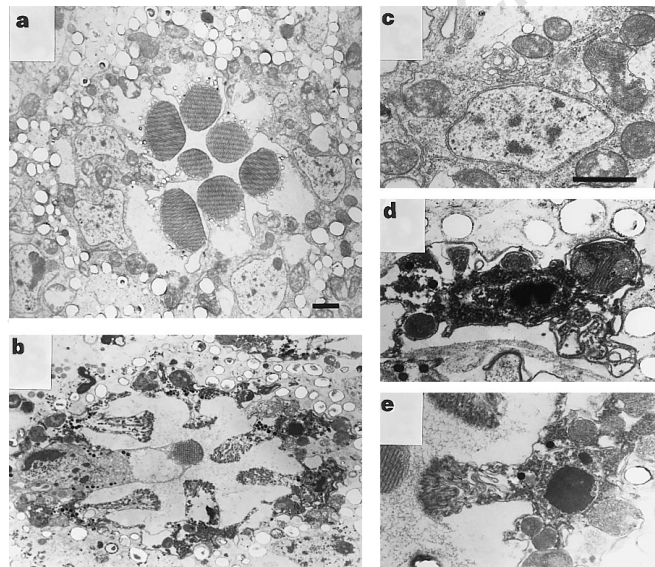
Figure 1 Photoreceptor cells in light-reared *ninaE*[RH27]/+ flies exhibit apoptotic morphology. **a**, Electron micrograph of a wild-type (Canton S) ommatidium. The membrane organelles at the centre of the ommatidium are the photoreceptor cell rhabdomeres, containing most of the cell's rhodopsin. **b**, An 8-week-old, light-reared *w*/+; +; *ninaE*[RH27]/+ fly ommatidium. Note the degeneration of the peripheral cells that express the mutant rhodopsin. The central photoreceptor cell, which expresses a different rhodopsin gene, looked normal here, but was degenerate in many ommatidia. **c**, A wild-type photoreceptor cell, with normal nuclear and mitochondrial morphology. **d**, **e**, High-magnification views of the cell bodies and subcellular organelles of the *w*/+; +; *ninaE*[RH27]/+ photoreceptor cells. Note the electron density of the cytoplasm and nuclei compared with the central photoreceptor cell, surrounding pigment cells, and wild-type cells (**a**). The normal spacing of the mitochondrial cristae indicates no lysis. Scale bars, 1 μm.
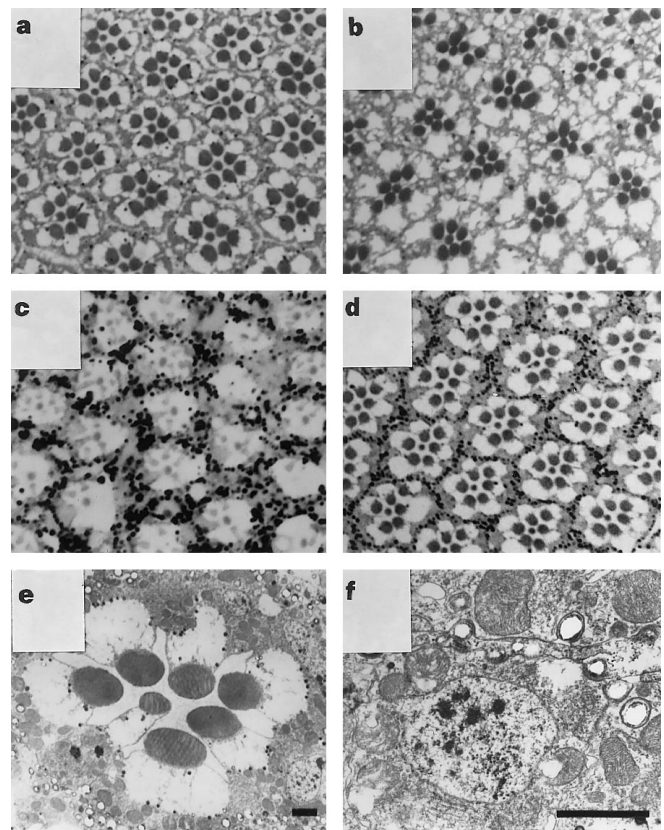
Figure 2 Retinal degeneration in *ninaE*[RH27]/+ flies is rescued by p35 expression. Light micrographs of retinal cross-sections of flies: **a**, wild type; **b**, dark-reared 4-week-old *w*/+; +; *ninaE*[RH27]/+; **c**, light-reared 8-week-old *w*/+; +; *ninaE*[RH27]/+; and **d**, light-reared 8-week-old *w*; +; *ninaE*[RH27]/*P*[*GMRp35 w*⁺]3-5. Scale bar, 15 μm. **e**, **f**, Electron micrographs of an ommatidium (**e**) and cell bodies and organelles (**f**) show normal morphology in the light-reared 8-week-old *w*; +; *ninaE*[RH27]/*P*[*GMRp35 w*⁺]3-5 fly retina. Scale bar, 1 μm.

**Table 1 Amplitudes of ERG response components in *rdgC* flies with and without p35.**

Light exposure	Genotype	N	ERG component (mV)		
			On	Sustained	Off
+	wild type	7	0.8 ± 0.3	5.4 ± 1.2	1.4 ± 0.8
+	*rdgC*	3	0.0 ± 0.0	0.0 ± 0.0	0.0 ± 0.0
+	*p35*; *rdgC*	6	0.6 ± 0.3	6.3 ± 1.7	0.8 ± 0.4
−	wild type	5	0.7 ± 0.4	7.0 ± 3.4	1.4 ± 0.4
−	*rdg C*	3	0.9 ± 0.4	8.2 ± 1.4	3.9 ± 1.2
−	*p35*; *rdgC*	3	1.6 ± 1.3	8.0 ± 2.5	2.4 ± 0.3

Amplitudes are ± s.e.m. Full genotypes are as indicated in Fig. 5.

effect of p35 on retinal degeneration, *ninaE*[RH27] and *rdgC*[306] flies were crossed with flies carrying single inserts of the transgene P[GMRp35][20], which confers eye-specific expression of p35 under the control of the GMR promoter[20]. Figure 2 shows representative light micrographs demonstrating that retinal degeneration was blocked in *ninaE*[RH27]/+ flies by the presence of the GMRp35 transgene, supporting the conclusion that photoreceptor cell death in this mutant occurs by apoptosis. The retinae of light-reared wild-type and young, dark-reared *ninaE*[RH27]/+ flies were indistinguishable (Fig. 2a, b), whereas those of light-reared *ninaE*[RH27]/+ flies 8 weeks old showed extensive loss of photorecep-tor cell rhabdomeres and bodies (Fig. 2c). However, the light-reared *ninaE*[RH27]/P[GMRp35] flies showed no degeneration at this age (Fig. 2d). Prevention of degeneration by p35 was also found when P[GMRp35] was inserted at a different site (not shown), indicating that the transgene's protective effect was not due to fortuitous disruption of a gene required for cell death. Electron micrographs of the *ninaE*[RH27]/P[GMRp35] fly retina shown in Fig. 2d demonstrate that its photoreceptor cells and organelles were indistinguishable from those of wild-type flies even at this level of resolution (Figs 1a, c, 2e, f). We also found that eye-specific expression of p35 prevented degeneration in *rdgC* flies (Fig. 3). Representative light micrographs of dark- and light-reared *rdgC* fly retinae show that degeneration followed the expected light-dependent pattern[12] (Fig. 3a, b). Yet light-reared P[GMRp35]; *rdgC* flies showed no degeneration, even at a later age (Fig. 3c). Antidromic illumination (not shown) also indicated no degeneration in P[GMRp35]; *rdgC* flies after 3 weeks in the light.

The ability of p35 to prevent retinal cell loss in these mutants allowed us to examine whether cells that would ordinarily commit to apoptosis can still function, despite the physiological stress that normally triggers death. To test for visual function in *ninaE*[RH27]/+ and *ninaE*[RH27]/P[GMRp35] flies, assays of a behaviour called the 'walking optomotor response' were used[27]. This assay measures the ability of a fly to discriminate and follow a rotating pattern of black and white stripes. Wild-type (Canton S) flies scored 91 ± 6 (Fig. 4), consistent with previous reports[27]. Light-reared *ninaE*[RH27]/+ flies showed normal optomotor responses up to 3 weeks of age (not shown), but by 5 weeks had lost all visual responsivity (Fig. 4). The visual responses of 5-week-old dark-reared *ninaE*[RH27]/+ flies were not significantly different from those of the wild type, indicating that the defective copy of the rhodopsin gene did not by itself block visual function. Most importantly, 5-week-old *ninaE*[RH27]/P[GMRp35] flies showed wild-type-like optomotor responses regardless of their light history.

Similar results were found when the effect of p35 expression on visual function was tested in *rdgC*[306] flies. In the optomotor response assay, *rdgC* flies gave highly variable responses even when reared in the dark, where no morphological degeneration occurs. This variation could be an effect of *rdgC* in the eye, or could be due to a function of the rdgC protein in the brain, where it is also expressed[13]. Electrophysiological assays were therefore used to test vision in *rdgC* mutant flies. Figure 5 and Table 1 show that, although dark-reared *rdgC* flies gave wild-type-like electroretinograms (ERGs), the light-reared *rdgC* flies showed no detectable ERG
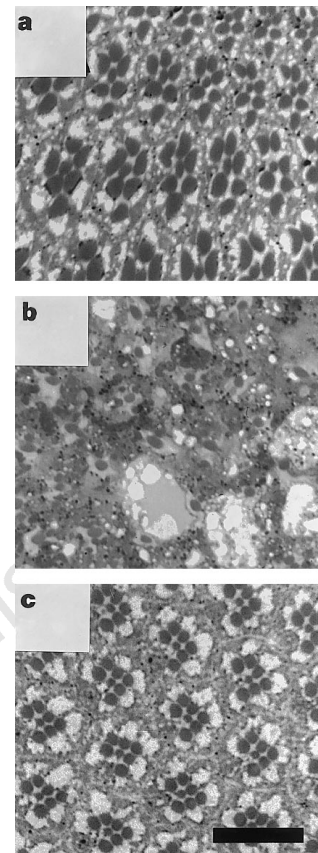
Figure 3 Retinal degeneration in *rdgC*[306] flies is rescued by p35 expression. Light micrographs of retinal cross-sections from flies: **a**, dark-reared 5-day-old +; +; *rdgC*[306], *cu*; **b**, light-reared 5-day-old +; +; *rdgC*[306], *cu*; and **c**, light-reared 11-day-old *w*; P[GMRp35 *w*+]2-1; *rdgC*[306], *cu*. Scale bar, 15 μm.
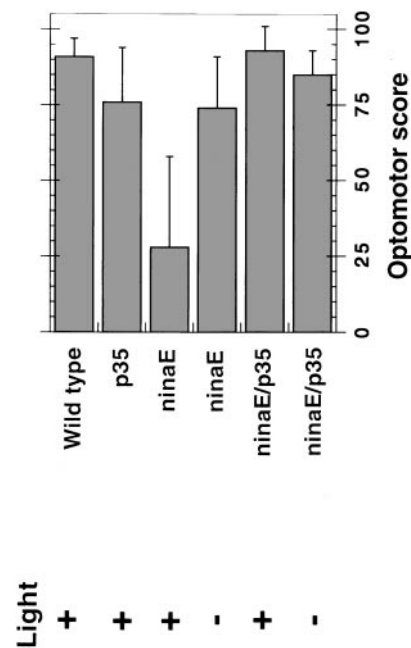
Figure 4 Optomotor responses in *ninaE*[RH27]/+ flies are rescued by p35 expression. The optomotor response scores (see text) are compared for flies raised for 5 weeks in either light (+) or dark (−). Wild type, Canton S flies; p35, transgenic flies expressing p35 in the retina (+; +; P[GMRp35 *w*+]3-5); *ninaE*, *ninaE* mutants (*w*/+; +; *ninaE*[RH27]/+); ninaE/p35, *ninaE* mutants expressing p35 in the retina (*w*; +; *ninaE*[RH27]/P[GMRp35 *w*+]3-5).

a Wild type

rdgC

P[GMRp35]; rdgC

3 s

b Wild type

rdgC

P[GMRp35]; rdgC

3 s
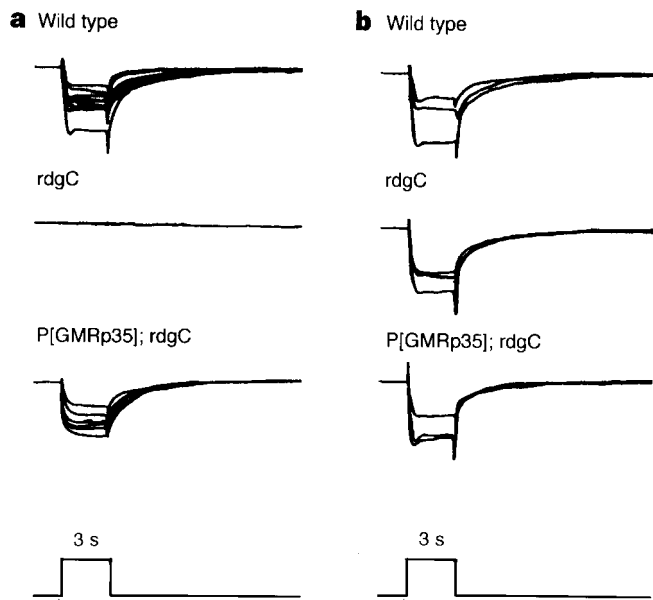
Figure 5 Electrophysiological responses in $rdgC^{306}$ flies are rescued by p35 expression. All flies were aged to 7 days under the conditions indicated. **a**, Light-reared flies; **b**, dark-reared flies. The electroretinograms (ERGs) of wild type, $rdgC$ and $P[GMRp35]$; $rdgC$ flies record light-induced changes in potential that are a summed function of the photoreceptor cell depolarizations caused by activation of rhodopsin signalling. The mean amplitudes of these responses ($\pm$ s.e.m.) are shown in Table 1. Wild type indicates Canton S flies; rdgC indicates +; +; $rdgC^{306}$, cu flies; p35; rdgC indicates w; $P[GMRp35\ w^+]2$-1; $rdgC^{306}$, cu flies.

responses by the same age. In contrast, light-reared $P[GMRp35]$; $rdgC$ flies showed ERG amplitudes within the range of the wild type. The apparent 'on' rates of light-stimulated depolarization were slightly slowed in light-reared $P[GMRp35]$; $rdgC$ flies than in their dark-reared siblings or other controls. The cause is unknown at present, but it may indicate some deceleration in downstream amplification[28] of the light signal. The visual signalling capacity of $P[GMRp35]$; $rdgC$ flies eliminates the possibility that p35 protein prevents retinal degeneration by blocking rhodopsin function or expression. Moreover, this result is consistent with previous observations that the GMR promoter itself does not impede the expression of other *glass*-responsive genes.

In conclusion, we have determined that photoreceptor cell death in both $ninaE^{RH27}$/+ and $rdgC$ light-dependent retinal degenerations proceeds by apoptosis and is inhibited by p35. This indicates that the activation of rhodopsin in these mutant backgrounds leads ultimately to caspase activation, and that caspase activation is required for degeneration. Our findings also made it possible to test whether the prevention of death would lead to restoration of function. It has been suggested that anti-apoptotic therapies may be useful for the treatment of various degenerative disorders[1]. However, no information was previously available as to whether cells rescued from apoptosis under such conditions can serve a useful function. Measurable visual function was preserved in the structurally rescued $ninaE^{RH27}$/+ and $rdgC$ mutant cells examined here, providing a strong rationale for further exploration of anti-apoptotic strategies in the treatment of degenerative disease. In particular, our results may provide a pointer for the effort to halt the progression of rhodopsin-mediated forms of RP. □

Methods

Fly strains and rearing conditions. Mutant w/+; +; $ninaE^{RH27}$/+, w; +; $ninaE^{RH27}$/$P[GMRp35\ w^+]3$-5, w; +/$P[GMRp35\ w^+]2$-1; $ninaE^{RH27}$/+ and +; $P[GMRp35\ w^+]2$-1; $rdgC$ flies were produced by standard genetic crosses from available fly stocks[10,12,20]. Light-reared flies were kept at 25 °C in continuous

fluorescent light beginning 1–2 days after eclosion. Dark-reared flies were treated identically except for the exclusion of light from their environment. Canton S flies were used as wild-type controls.

Histology. Flies were decapitated under anaesthesia and the heads fixed in 2.5% glutaradehyde in 0.1 M sodium cacodylate, pH 7.2, on ice for 30 min. OsO_4 was then added to a final concentration of 1% and fixation continued for 30 min. Glutaraldehyde and OsO_4 were removed and the heads fixed for 2 h in fresh 1% OsO_4 in the same buffer, rinsed with ice-cold water, stained in 1% aqueous uranyl acetate for 2 h, rinsed again with water, dehydrated through an ethanol series and propylene oxide, and embedded in Spurr's resin. Transverse semithin (0.5–1 μm) sections were stained with methylene blue and toluidine blue for light microscopy. Transverse thin (50 nm) sections were post-stained with uranyl acetate and lead citrate for transmission electron microscopy at 80 kV.

Walking optomotor assays. The behavioural response of flies to a moving visual field was assayed as described[27]. Normal flies attempted to stabilize their visual field in this assay by walking or turning in the direction of a rotating drum of black and white stripes. Behaviour was scored as the number of times each fly walked across a quadrant line in the same direction as the rotating stripes, divided by the number of times it walked in the opposite direction, multiplied by 100. Between 4 and 10 flies were tested per genotype, age and rearing condition. Every fly was tested in three successive trials, each consisting of a 1-min clockwise drum rotation followed by a 1-min anticlockwise rotation and a per-trial mean score calculated. Optomotor response scores were calculated as the average of the mean individual fly responses ($\pm$ s.e.m.) for that genotype, age and rearing condition. A score of 100 signifies that flies walk in the direction of visual field rotation 100% of the time. A score of 50% indicates that walking direction does not correlate with the direction of field rotation. Flies that lack functional photoreceptor cells and flies with impaired higher-order processing can both yield the latter score. Therefore, dark- and light-reared flies of the same age were tested to control for cognitive dysfunction unrelated to illumination history.

Electroretinograms. The electroretinograms (ERGs) of wild-type (Canton S), mutant +; +; $rdgC^{306}$, cu and w; $P[GMRp35]2$-1; $rdgC^{306}$, cu flies were obtained as described[27]. A measuring electrode was inserted through the lens layer of one eye of each immobilized live fly, and a reference electrode was inserted through the cuticle at the back of the head. After dark adaptation for 3 min, the fly was illuminated with individual 3-s pulses of white light from a fibre-optic light source connected to a standard pulse generator. Electrode output was transmitted through a Grass P18 battery-operated preamplifier to a strip-chart recorder. All ERG measurements on mutant flies were bracketed by measurements on wild-type flies. Three recordings were taken per fly and 3–7 flies were tested per genotype, age and rearing condition. Each of the superimposed traces shows a sample ERG response obtained from one fly. Intra-fly means of the response component amplitudes were used to calculate the mean inter-fly response amplitudes ($\pm$ s.e.m.) in Table 1. Standard deviations of the mean of the intra-fly ERG response amplitudes were typically less than 10%.

1. Thompson, C. B. Apoptosis in the pathogenesis and treatment of disease. *Science* **267,** 1456–1462 (1995).
2. Steller, H. Mechanisms and genes of cellular suicide. *Science* **267,** 1445–1449 (1995).
3. Hengartner, M. O. & Horvitz, H. R. Programmed cell death in *Caenorhabditis elegans. Curr. Opin. Genet. Dev.* **4,** 581–586 (1994).
4. Jacobson, M. D., Weil, M. & Raff, M. C. Programmed cell death in animal development. *Cell* **88,** 347–354 (1997).
5. Chang, G. Q., Hao, Y. & Wong, F. Apoptosis: final common pathway of photoreceptor death in rd, rds, and rhodopsin mutant mice. *Neuron* **11,** 595–605 (1993).
6. Portera-Cailliau, C., Sung, C. H., Nathans, J. & Adler, R. Apoptotic photoreceptor cell death in mouse models of retinitis pigmentosa. *Proc. Natl Acad. Sci. USA* **91,** 974–978 (1994).
7. Nickells, R. W. & Zack, D. J. Apoptosis in ocular disease: a molecular overview. *Opthal. Genet.* **17,** 145–165 (1996).
8. Humphries, P., Farrar, G. J., Kenna, P. & McWilliam, P. Retinitis pigmentosa: genetic mapping in X-linked and autosomal forms of the disease. *Clin. Genet.* **38,** 1–13 (1990).
9. Colley, N. J., Cassill, J. A., Baker, E. K. & Zuker, C. S. Defective intracellular transport is the molecular basis of rhodopsin-dependent dominant retinal degeneration. *Proc. Natl Acad. Sci. USA* **92,** 3070–3074 (1995).
10. Kurada, P. & O'Tousa, J. E. Retinal degeneration caused by dominant mutations in *Drosophila. Neuron* **14,** 571–579 (1995).
11. Richards, J. E., Scott, K. M. & Sieving, P. A. Disruption of conserved rhodopsin disulfide bond by Cys187Tyr mutation causes early and severe autosomal dominant retinitis pigmentosa. *Opthalmology* **102,** 669–677 (1995).
12. Steele, F. & O'Tousa, J. E. Rhodopsin activation causes retinal degeneration in *Drosophila rdgC* mutant. *Neuron* **4,** 883–890 (1990).

13. Steele, F. R., Washburn, T., Rieger, R. & O'Tousa, J. E. *Drosophila* retinal degeneration C (rdgC) encodes a novel serine/threonine protein phosphatase. *Cell* **69**, 669–676 (1992).
14. Byk, T., Bar-Yaacov, M., Doza, Y. N., Minke, B. & Selinger, Z. Regulatory arrestin cycle secures the fidelity and maintenance of the fly photoreceptor cell. *Proc. Natl Acad. Sci. USA* **90**, 1907–1911 (1993).
15. Dryja, T. P. Rhodopsin and autosomal dominant retinitis pigmentosa. *Eye* **6**, 1–10 (1992).
16. Cohen, G. M. Caspases: the executioners of apoptosis. *Biochem. J.* **326**, 1–16 (1997).
17. Xue, D. & Horvitz, H. R. Inhibition of the *Caenorhabditis elegans* cell-death protease CED-3 by a CED-3 cleavage site in baenlovirus p35 protein. *Nature* **377**, 248–251 (1995).
18. Bump, N. J. *et al.* Inhibition of ICE family proteases by baculovirus antiapoptotic protein p35. *Science* **269**, 1885–1888 (1995).
19. Clem, R. J. & Miller, L. K. Control of programmed cell death by the baculovirus genes p35 and iap. *Mol. Cell. Biol.* **14**, 5212–5222 (1994).
20. Hay, B. A., Wolff, T. & Rubin, G. M. Expression of baculovirus p35 prevents cell death in *Drosophila*. *Development* **120**, 2121–2129 (1994).
21. Grether, M. E., Abrams, J. M., Agapite, J., White, K. & Steller, H. The head involution defective gene of *Drosophila melanogaster* functions in programmed cell death. *Genes Dev.* **9**, 1694–1708 (1995).
22. White, K.,Tahaoglu, E. & Steller, H. Cell killing by the *Drosophila* gene reaper. *Science* **271**, 805–807 (1996).
23. Sugimoto, A., Friesen, P. D. & Rothman, J. H. Baculovirus p35 prevents developmentally programmed cell death and rescues a ced-9 mutant in the nematode *Caenorhabditis elegans*. *EMBO J.* **13**, 2023–2028 (1994).
24. Rabizadeh, S., La Count, D. J., Friesen, P. D. & Bredeson, D. E. Expression of the baculovirus p35 gene inhibits mammalian neural cell death. *J. Neurochem.* **61**, 2318–2321 (1993).
25. Beidler, D. R., Tewari, M., Friesen, P. D., Poirier, G. & Dixit, V. M. The baculovirus p35 protein inhibits Fas- and tumor necrosis factor-induced apoptosis. *J. Biol. Chem.* **270**, 16526–16528 (1995).
26. Martinou, I. *et al.* Viral proteins E1B19K and p35 protect sympathetic neurons from cell death induced by NGF deprivation. *J. Cell Biol.* **128**, 201–208 (1995).
27. Rendahl, K. G., Jones, K. R., Kulkarni, S. J., Bagully, S. H. & Hall, J. C. The dissonance mutation at the no-on-transient-A locus of *D. melanogaster*: genetic control of courtship song and visual behaviors by a protein with putative RNA-binding motifs. *J. Neurosci.* **12**, 390–407 (1992).
28. Ranganathan, R., Malicki, D. M. & Zuker, C. S. Signal transduction in *Drosophila* photoreceptors. *Annu. Rev. Neurosci.* **18**, 283–317 (1995).
29. Wyllie, A. H. Apoptosis and carcinogenesis. *Eur. J. Cell Biol.* **73**, 189–197 (1997).

CD40 ligand on activated platelets triggers an inflammatory reaction of endothelial cells

Volker Henn*†, **Joseph R. Slupsky**†‡, **Michael Gräfe**§,
Ioannis Anagnostopoulos‖, **Reinhold Förster**¶,
Gert Müller-Berghaus‡ & **Richard A. Kroczek***

* *Molecular Immunology, Robert Koch-Institute, 13353 Berlin, Germany*
‡ *Haemostasis Research Unit, Max-Planck-Institut für Physiologie und Klinische Forschung, Kerckhoff-Klinik, 61231 Bad Nauheim, Germany*
§ *Deutsches Herzzentrum, Augustenburger Platz 1, 13353 Berlin, Germany*
‖ *Institute of Pathology, Klinikum Benjamin Franklin, Freie Universität Berlin, Germany*
¶ *Max-Delbrück-Center for Molecular Medicine, 13122 Berlin, Germany*
† *These authors contributed equally to this work.*

....

CD40 ligand (CD40L, CD154), a transmembrane protein structurally related to the cytokine TNF-α, was originally identified on stimulated CD4^{+} T cells[1–3], and later on stimulated mast cells and basophils[4]. Interaction of CD40L on T cells with CD40 on B cells is of paramount importance for the development and function of the humoral immune system[5]. CD40 is not only constitutively present on B cells, but it is also found on monocytes, macrophages and endothelial cells, suggesting that CD40L has a broader function *in vivo*. We now report that platelets express CD40L within seconds of activation *in vitro* and in the process of thrombus formation *in vivo*. Like TNF-α and interleukin-1, CD40L on platelets induces endothelial cells to secrete chemokines and to express adhesion molecules, thereby generating signals for the recruitment and extravasation of leukocytes at the site of injury. Our results indicate that platelets are not only involved in haemostasis but that they also directly initiate an inflammatory response of the vessel wall.

Human platelets were analysed by flow cytometry for the expression of CD40L on the cell surface. CD40L was not detectable on unstimulated platelets, but activation of platelets by the agonist thrombin (monitored by staining for CD63) resulted in maximal expression of CD40L within one minute (Fig. 1); thereafter, CD40L levels gradually declined. CD40L was also released in the presence of collagen or ADP plus adrenaline as agonists (results not shown). These experiments demonstrate that preformed CD40L is stored in platelets and is translocated to the cell surface as part of the 'basic platelet reaction' in which rapid upregulation of CD63, P-selectin, and several other proteins on the cell surface is accompanied by the release of soluble mediators from intracellular granules[6,7].

Immunoprecipitation with the monoclonal antibody TRAP1 indicated that the 33K and 28K transmembrane forms of human CD40L[8] are indistinguishable in platelets and activated CD4^{+} T cells (Fig. 2a). The ability of platelet CD40L to bind CD40 was verified by using a soluble CD40-immunoglobulin (CD40-Ig) chimaeric reagent for immunoprecipitation (Fig. 2b). Sequencing of the CD40L complementary DNA obtained from platelets and the megakaryoblastic lines MEG-01 and UT-7 by reverse transcription followed by polymerase chain reaction (RT-PCR) revealed identity to the CD40L sequence from T cells[2] (not shown). The CD40L molecule on platelets is thus identical in structure and specificity to the CD40L expressed on activated CD4^{+} T cells.
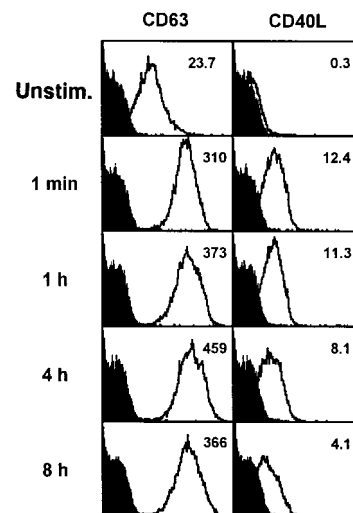
Figure 1 Expression of CD40L on activated platelets. Platelets were either left unstimulated or were stimulated with 0.2 U ml^{−1} of human thrombin for the indicated times, fixed, and analysed by flow cytometry for expression of CD63 (or P-selectin; results not shown) and CD40L. The background signal is shown in black; inset numbers indicate the net geometrical mean of fluorescence of the cell population analysed. Unstim., unstimulated.
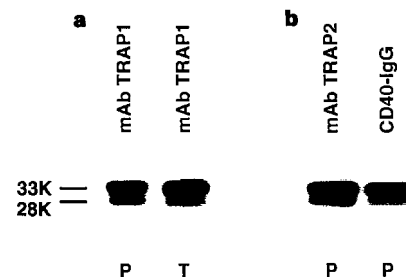
Figure 2 CD40L on platelets has the same structure and specificity as CD40L on activated CD4^{+} T cells. **a**, Immunoprecipitates of CD40L from platelets and obtained with TRAP1, or **b**, immunoprecipitates with a chimaeric CD40–Ig reagent (TRAP2 antibody was used for comparison) were analysed by western blotting with a CD40L-specific antiserum. P, platelets; T, T cells.